

# Dental Biometrics: Human Identification Using Dental Radiographs

## (To appear in AVBPA2003) \*

Anil K. Jain, Hong Chen, and Silviu Minut

Department of Computer Science, Michigan State University, East Lansing, MI 48824  
{jain, chenhon2, minutsil}@cse.msu.edu

**Abstract.** The goal of forensic dentistry is to identify people based on their dental records, mainly as radiograph images. In this paper we attempt to set forth the foundations of a biometric system for semi-automatic processing and matching of dental images, with the final goal of human identification. Given a dental record, usually as a postmortem (PM) radiograph, we need to search the database of antemortem (AM) radiographs to determine the identity of the person associated with the PM image. We use a semi-automatic method to extract shapes of the teeth from the AM and PM radiographs, and find the affine transform that best fits the shapes in the PM image to those in the AM images. A ranking of matching scores is generated based on the distance between the AM and PM tooth shapes. Initial experimental results on a small database of radiographs indicate that matching dental images based on tooth shapes and their relative positions is a feasible method for human identification.

## 1. Introduction

The main purpose of forensic dentistry is to identify deceased individuals for whom other means of identification (e.g., fingerprint, face, etc) [3] are not available. In general, there must be a presumptive (or tentative) identity for the deceased, so that postmortem (PM) dental records can be compared against specific antemortem (AM) records (See Fig. 1). A manual comparison between the AM and PM records is based on a systematic dental chart completed by some forensic experts [6][5]. In this chart, a number of distinctive features are noted for each tooth individually. These features include properties of the teeth (e.g., tooth present/not present, crown and root morphology and pathology and dental restorations), periodontal tissue features, and anatomical features. Depending on the number of matches, the forensic expert rejects or confirms the tentative identity.

Unlike other biometric characteristics (e.g., fingerprints, iris, etc.), dental identification is complicated by the fact that dental features do change over time. The teeth can change appearance, or can be missing altogether, as a result of dental work or accidents occurring after the AM records are taken. In fact, for this very reason, although

---

\* This research was partially supported by the National Science Foundation under grant EIA-0131079.

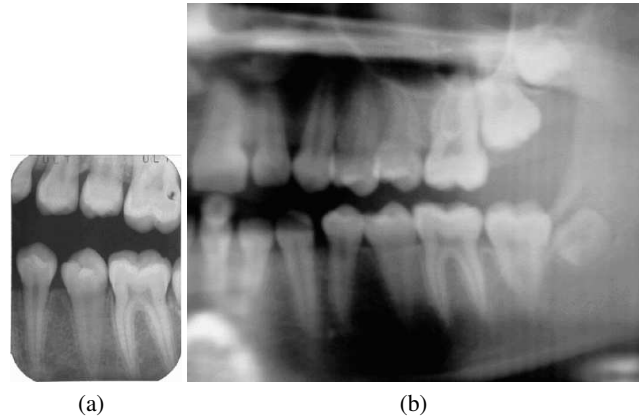


**Fig. 1.** Postmortem (a) and antemortem (b) dental radiographs.

accepted in a court of law, dental based identification is considered less reliable than other biometric methods. But in certain cases (e.g., victims in a major fire), this may be the only available biometric method.

From a pattern recognition and computer vision standpoint, the problem of person identification based on dental records can be cast as an image matching and retrieval problem: given a dental image (usually a PM radiograph), we must search the database to find an AM radiograph that best matches with this PM record. In this paper, we use the terms *PM image* and *query image*, and *AM image* and *database image*, interchangeably. At a first glance, this problem seems more constrained than the generic object detection and object recognition problem. However, building a dental chart with distinctive features for each individual tooth (as human experts do) is extremely difficult, because the system must detect and classify each tooth before it can process them. To label a single tooth as “cuspid”, “first molar”, “second molar”, etc. in a given image, is very difficult for several reasons. One issue is the fact that the *coarse* shape of a tooth is not unique. For instance, all pre-molars have roughly the same shape, as do all molars and all incisors. Furthermore, the system must decide when to rely upon, and when to ignore the dental work (e.g., fillings and artificial crowns).

## 2. System Overview

Given the difficulty of building a dental chart with distinctive features for each of the 32 teeth, one would expect to obtain better matching results if we match several teeth simultaneously, in the AM and PM images. The relative positions of the teeth with respect to each other should rule out the inherent ambiguities that arise when one tooth at a time is matched, irrespective of the other teeth. The diagram in Figure 2 presents the main modules of our system. The shape extraction module extracts the shapes of the teeth in the database radiographs and query images. The matching module matches the shapes from the query image to those from the database images. Then a ranking is produced to show the best matching(s) in the database. In the subsequent sections we present the details of each of these stages.

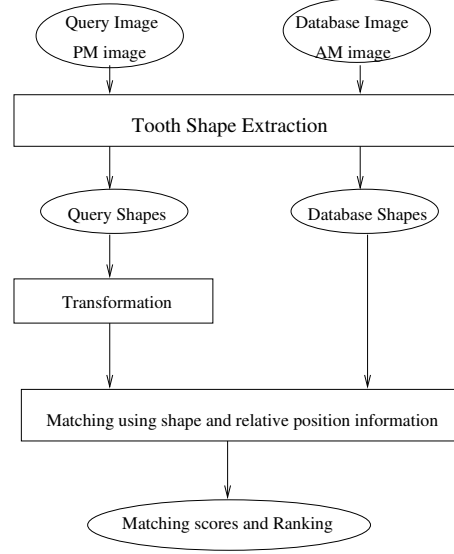


**Fig. 2.** The logical modules of the dental biometrics system.

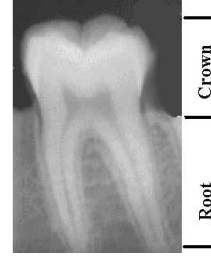


**Fig. 3.** Two parts of a tooth: crown and root.

### 3. Shape Extraction

A tooth includes two parts: the upper part is called the *crown*, which is above the gum-line, and the lower part is called the *root*, which sits in the bone below the gum (see Fig. 3). Because of the bone and the soft tissue, the root of the tooth is not very visible in the radiographs. We divide the shape extraction procedure into two stages: extraction of the crown's shape and the extraction of the root's shape. Since the crown has a higher contrast with the background than the root, we extract the shape of the crown first. Then based on the contour of the crown, the shape of the root is extracted.

Dental radiographs often do not have high contrast, which makes it very difficult to automatically extract the boundaries of teeth. To simplify the shape extraction, we manually select a rectangular region  $R$  and a point  $c$  in the input image,  $I$  (Fig. 4(a)).  $R$  is a region containing the tooth and the point  $c$  is inside the crown of the tooth, which is called the *Crown Center*. First, we compute the gradient image,  $|\nabla I|$ , of the input image,  $I$ , as

$$|\nabla I(x, y)| = \sqrt{(I(x, y) - I(x, y - 1))^2 + (I(x, y) - I(x - 1, y))^2}. \quad (1)$$

Due to the proximity of the neighboring teeth, there is some *interference* between the edges of a tooth and the edges of adjacent teeth. To solve this problem, we define an auxiliary image,  $M$ , by

$$M(x, y) = B(x, y)|\nabla I(x, y)|, \quad (2)$$

where

$$B(x, y) = \begin{cases} 0 & \text{if } \nabla I(x, y) \cdot \mathbf{E}(x, y) < 0 \\ 1 & \text{otherwise,} \end{cases}$$

and  $\nabla I(x, y)$  is the gradient direction vector at  $(x, y)$ ,  $\mathbf{E}(x, y)$  is a vector from Crown Center  $c$  to  $(x, y)$ , and  $\cdot$  denotes the dot product (see Fig. 5(a)). Note that when  $\mathbf{E}(x, y)$  and  $\nabla I(x, y)$  form an acute angle,  $B(x, y)$  equals 1; otherwise,  $B(x, y)$  equals 0. As a result, the effect of the edges of the neighboring teeth in computing the gradient is greatly decreased (Fig. 4(c)).

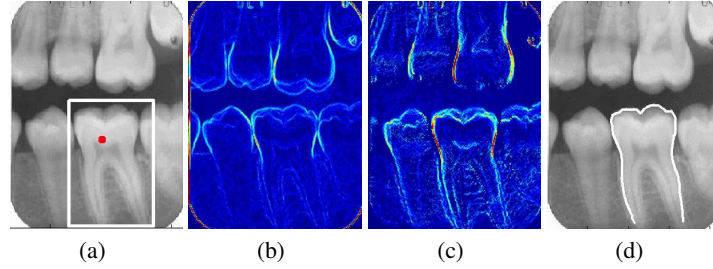


**Fig. 4.** Removing the interference caused by the neighboring teeth. (a) Input image, in which a rectangular region and the crown center are selected; (b) Gradient image,  $|\nabla I|$ ; (c) Gradient image after removing interference,  $M$ ; (d) Extracted tooth shape.

From the crown center, we make a radial scan of the crown. The edge of the crown should be somewhere along this radial line. We sort all the points on the radial line in terms of  $M(x, y)$ , and record the three largest ones. If we draw a sufficiently large number of radial lines, then a list of edge candidates is produced (see Fig. 5(b)). Let  $\bar{M}$  be the mean of all the recorded  $M(x, y)$  values. We define the reliability,  $R(x, y)$ , of each edge candidate  $(x, y)$  by

$$R(x, y) = \begin{cases} e^{-\alpha(M(x, y) - \bar{M})^2} & \text{if } M(x, y) < \bar{M}, \\ 1 & \text{if } M(x, y) \geq \bar{M}, \end{cases} \quad (3)$$

where  $\alpha$  is a constant to prevent  $R(x, y)$  from decaying too fast. Along each radial line, the point with the largest reliability is selected to be an edge point.

Once the shape of the crown is extracted, we traverse from the two ends of the crown's shape to find the contour of the root. The left end of the crown is set as the first point on the left contour of the root, and the right end of the crown is the first point of the right contour. Then we determine the position of each new contour point by the position of the previous contour point and its own *context*. As a measurement of the *context*, we define two attributes at each point:  $I_{inner}$  for the *inner intensity* of the contour and  $I_{outer}$  for the *outer intensity*. For the left contour, *inner intensity* is the average intensity of a small region to the right of the contour, and *outer intensity* is the average intensity of a small region to the left of the contour; for the right contour, it's just the opposite (see Fig 5(c)). Our aim is to find the root contour that maximizes the

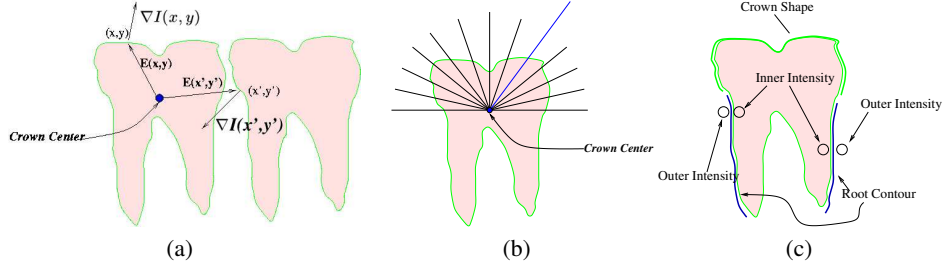


**Fig. 5.** Crown shape and root contour extraction. (a) Definition of vectors  $\nabla I(x, y)$  and  $D(x, y)$ . The gradient at  $(x, y)$  will be retained while the gradient at  $(x', y')$  will be set to zero; (b) Edges along radial scans; (c) Inner intensity and outer intensity.

difference between  $I_{inner}$  and  $I_{outer}$ . In other words, if the  $i$ th point on the left/right root contour is  $(x_i, y_i)$ , the  $(i + 1)$ th point  $(x_{i+1}, y_{i+1})$  is computed iteratively as:

$$\begin{aligned} x_{i+1} &= \max_{x_i - r \leq x \leq x_i + r} (I_{inner} - I_{outer}), \\ y_{i+1} &= y_i + h, \end{aligned} \quad (4)$$

where  $r$  is the radius of the search space and  $h$  is the increment in the vertical position for each new point. Since the information regarding the tooth template is not taken into consideration, small errors are possible.

#### 4. Shape Fitting

The shapes extracted from the query image must be matched to the shapes extracted from the database images. One of the main difficulties in matching AM and PM images is due to the fact that they were taken at different times often as long as several years. Thus the view points are usually slightly different, which causes an *affine transformation* between the two images that must be considered prior to shape fitting.

We confine ourselves with a subclass of the affine transformation. In particular, we do not consider the shear transformation, because the shear is negligible in AM and PM images. Thus the affine transformation,  $T$ , is a function of the form

$$T : \mathbf{R}^2 \longrightarrow \mathbf{R}^2, \quad T(P) = A \cdot P + \tau, \quad (5)$$

where  $P = (x, y)^t$  represents a point in the query shape,  $T(P)$  is the result of applying the transformation  $T$  on  $P$ ,  $A$  is the transformation matrix, and  $\tau$  is the translation vector. The parameters  $A$  and  $\tau$  can be represented as:

$$A = \begin{pmatrix} \cos\theta & \sin\theta \\ -\sin\theta & \cos\theta \end{pmatrix} \cdot \begin{pmatrix} S_x & 0 \\ 0 & S_y \end{pmatrix}, \quad \tau = \begin{pmatrix} \tau_x \\ \tau_y \end{pmatrix}. \quad (6)$$

There are a total of 5 parameters in the transformation  $T$ ,  $\{\theta, S_x, S_y, \tau_x, \tau_y\}$ , where  $\theta$  is the rotation angle,  $S_x$  and  $S_y$  are vertical and horizontal scale factors, and  $\tau_x$  and  $\tau_y$  are vertical and horizontal translations. They are optimized for best fitting between the transformed query shape and the database shape.

Given a query image, from every database image we generate several sub-images, each containing the same number of teeth as the query image. The teeth in query image and database sub-images are labeled as 1,2,..., from left to right. Then teeth with the same label in query and database subimage form a pair.

For each pair, we define the *matching distance*  $MD$  that needs to be minimized:

$$MD(T) = \sum_{each\ pairs\ of\ shapes} D(T),$$

$$D(T) = \sum_{P(i) \in query\ shape} \{ \min_{P'(j) \in database\ shape} \|P(i) - T(P'(j))\| \}. \quad (7)$$

So,  $D(T)$  is the distance between a pair of teeth, and  $MD(T)$  is the summation of all  $D(T)$  in a query.

By finding the *tightest fitting rectangle* for the groups of query shapes and database shapes, the parameters in the transformation  $T$  are initialized as:

$$\theta = \theta_q - \theta_d, \quad S_x = W_q/W_d, \quad S_y = S_x, \quad \tau_x = Cq_x - Cd_x, \quad \tau_y = Cq_y - Cd_y, \quad (8)$$

where  $\theta_q$  and  $\theta_d$  are the orientations of lengths of the tightest fitting rectangles for the query shapes and the database shapes respectively,  $W_q$  and  $W_d$  are the widths of the rectangles, and  $(Cq_x, Cq_y)$  and  $(Cd_x, Cd_y)$  are the centers of the rectangles. A Sequential Quadratic Programming (SQP) method [2] is applied for optimization. Ranges of the parameter values are set to properly guide the optimization procedure. Finally, a ranking of database images is generated with respect to the matching distance,  $MD(T)$ .

## 5. Experimental Results

The proposed identification method has been applied to 38 query images for retrieval from a database, which contains 130 AM images. In each query image, we divide the teeth into two groups: upper set of teeth and lower set of teeth. The teeth in the same group will not change their relative positions, while teeth from the two groups will probably change their relative positions because of the opening and closing of the mouth. So, we match the two groups separately.

Figure 6 shows an example of a query image matched with a genuine and an impostor database image. Among the 38 queries, 25 true PM images were correctly retrieved. For the remaining 13 queries, 5 of them were among the top 2 retrieved images and 9 were among the top 5 retrieved images. The performance curve is shown in Figure 7. The 13 query images were not correctly matched because of (i) poor quality of images so that teeth shapes were not reliably extracted, (ii) teeth were only partially visible, and (iii) the inherent similarity between different teeth shapes.

## 6 Conclusions and Future Work

A new semi-automatic method of human identification with dental radiographs is proposed. Preliminary experiments on a small database indicate that this is a feasible approach. However, in some cases, it is difficult to apply the proposed method because the images are very blurred (Fig. 8(a)), or the query shape is partially occluded so there is not enough information available to characterize the teeth (Fig. 8(b)). Fortunately, the

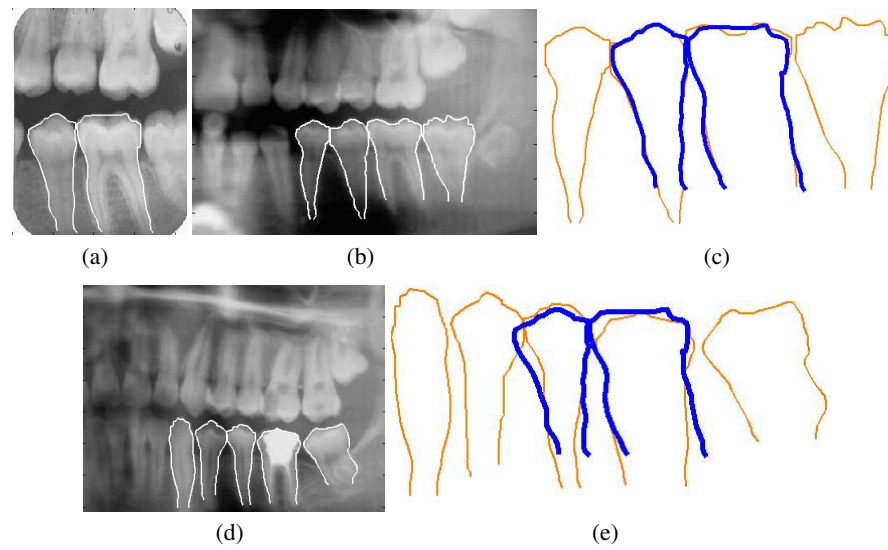


**Fig. 6.** An example of matching. (a) Query image with 2 lower teeth extracted; (b) True AM image from the database with 4 lower tooth shapes extracted; (c) Query shapes and true matching shapes overlaid ( $MD = 4.22$ ); (d) Imposter AM image with 5 lower tooth shapes extracted; (e) Query shapes and the imposter's shapes overlaid ( $MD = 27.57$ ). The gray lines represent the shapes in the database; the black lines represent the query shapes after transformation.

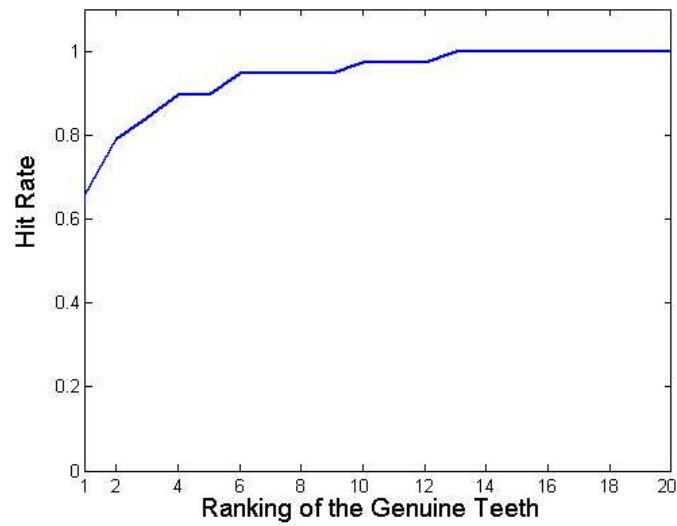


**Fig. 7.** Performance curve.

radiographs not only give us the information about the shape of the teeth, but also other information such as the artificial prothesis of the teeth, the striae patterns [1] and trabecular patterns [4], etc. Future work will involve utilizing this information to improve the reliability of person identification with dental images. We are also in the process of developing an image restoration algorithm to handle poor quality radiographs and obtaining a large database of dental radiographs to rigorously evaluate our algorithm.

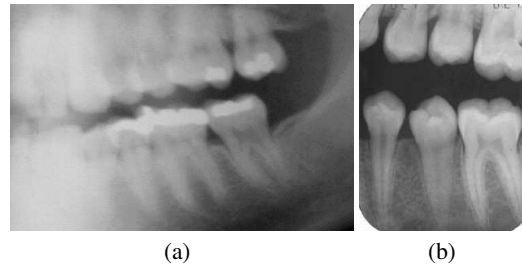


**Fig. 8.** Examples of images where the proposed matching approach fails. (a) The image is too blurred for reliable shape extraction; (b) The upper teeth are only partially visible.

## References

1. Marcelo Cavalcanti, Axel Ruprecht, William Johnson, Southard Thomas, Jane Jakobsen, and Sao Paulo. Oral and maxillofacial radiology. *Oral Surg Oral Med Oral Pathol*, volume 88:pages 353–357, 1999.
2. S.P. Han. A globally convergent method for nonlinear programming. *Journal of Optimization Theory and Applications*, volume 22:pages 297, 1977.
3. Anil Jain, Ruud Bolle, and Sharath Pankanti. *Biotmetrics–Personal Identification in Networked Society*. Kluwer Academic Publishers, 1999.
4. Greth Jonasson and Gudrun Bankvall. Estimation of skeletal bone mineral density by means of the trabecular pattern of the alveolar bone, its interdental thickness, and the bone mass of the mandible. *Oral Surg Oral Med Oral Pathol Oral Radiol Endod*, volume 92:pages 346–352, 2001.
5. American Board of Forensic Odontology. Body identification guidelines. *J. Am. Dent. Assoc.*, vol.125:pages 1244–1254, 1994.
6. I. A. Pretty and D. Sweet. A look at forensic dentistry - part 1: The role of teeth in the determination of human identity. *British Dental Journal*, volume 190(7):pages 359–366, April 2001.